UC Riverside

UCR Honors Capstones 2019-2020

Title

EphA4 Antagonists Stabilized by Non-Covalent Intramolecular Interactions

Permalink

https://escholarship.org/uc/item/7b38x8m9

Author

Pagett, James

Publication Date

2021-01-11

Data Availability

The data associated with this publication are within the manuscript.

By

A capstone project submitted for
Graduation with University Honors

University Honors
University of California, Riverside

APPROVED

_____
Dr.
Department of

_____
Dr. Richard Cardullo, Howard H Hays Jr. Chair, University Honors

Abstract

Acknowledgements

  I would like to extend my utmost thanks to my faculty mentor, Dr. Maurizio Pellecchia, as well as project scientists Dr. Luca Gambini and Dr. Carlo Baggio for their excellent guidance through this project. Their close mentorship transformed the final year of my undergraduate career into a rewarding experience of real, meaningful research that will leave an everlasting impact in my future as an aspiring scientist.

  Additionally, I would like to thank my closest peers, especially Dev Tanna and Andrew Gomez, who through the past four years have held me to my potential – always in good, competitive spirit. Finally, I need to thank my entire family for their unconditional support. Mom and Dad, thank you for your constant availability no matter the crisis and for securing me financially. Jordan, thank you for catalyzing my application to UC Riverside – No other campus would have fostered the environment that helped me grow into who I am today. Jared, thank you for inspiring me to pursue science with passion and vigor. Grandma and Papa, your love all the way from Rocklin always helped me feel right at home 450 miles away. I would not be where I am now if it were not for any of you.

Table of Contents

Introduction

In a highly influential proof-of-concept study, EphA4 was shown to be a disease modifier in amyotrophic lateral sclerosis, or ALS (Van Hoecke et al., 2012). In SOD1 mutant zebrafish models, they found that heterozygous deletion of the Rtk2 gene, the zebrafish equivalent of human EphA4, resulted in great improvements in motor coordination and overall survivability. It was also shown that introducing an antagonistic agent for EphA4 was implicated with delaying disease onset. Additional insight was necessary to address the legitimate role of EphA4 antagonists and ALS. The discovery that EphA4 expression is inversely correlated with ALS disease onset in humans led many scientists to pursue EphA4 targeting ligands as potential means of slowing the progression of ALS. More recently, EphA4 signaling activation was also implicated in the onset and progression of Alzheimer's disease (AD) (Poppe et al., 2019). In particular, loss of EphA4 signaling in AD mice models resulted in improved social memory without affecting other cognitive functions, suggesting that EphA4 antagonists may have a therapeutic benefit for AD patients. The detailed mechanisms of EphA4 signaling in these pathologies is complex, involving bi-directional signaling in cell-cell contacts (Pasquale, 2008), and are not yet fully elucidated. However, there seems to be a consensus that EphA4 agonistic agents may be beneficial as ALS therapeutics while antagonistic agents may be beneficial for the treatment of AD.

Two prominent antagonistic peptides selective for EphA4 were discovered via phage display, denoted as KYL (KYLPYWPVLSSL) and the cyclic peptide APY (APY<u>C</u>VYRGSWS<u>C</u>; cyclized via a disulfide bond between two the two underlined Cys residues) (Murai et al., 2003). The linear peptide KYL showed the highest binding affinity of the two (1 µM), however APY held the most potential for optimizing binding affinity due to an

intramolecular disulfide bond between its two cysteine residues that stabilize the peptide into its bioactive ß-hairpin conformation. Follow-up studies produced far more potent APY derivatives, notably APY-d3, through optimizing the formation of the ß-hairpin (Olson et al., 2016). These potent EphA4 antagonists were geared toward ALS implications, however recent research has shown that an EphA4 agonist may be a more optimal route of slowing ALS progression.

A short peptide-mimetic recently reported by the Pellecchia Laboratory, denoted 123C4, was shown to activate the EphA4 receptor and induce receptor endocytosis (Wu et al., 2017). Triggering endocytosis of EphA4 prevents interaction of the receptor to the endogenous ligand ephrin-B2, which is thought to prevent the repair of motor neurons in those with ALS. This data suggests that it is the reverse signaling induced by the ligand ephrin-B2 rather than the EphA4 receptor forward signaling that is correlated with the progression of ALS.

However, recent research has shown that the EphA4/c-Abl signaling pathway plays a significant role in the decline of dendritic spine density in those with Alzeimer's disease (AD) (Vargas et al., 2018). Soluble amyloid beta oligomers (AßOs) found in AD models hyperactivate EphA4 which in turn activates c-Abl, another tyrosine-protein kinase responsible for a multitude of downstream degenerative effects on the synapse. Thus, introducing antagonistic agents to outcompete the binding of AßOs to EphA4 may be a viable route of diminishing the retraction of dendritic spines in AD.

The EphA4 antagonist APY-d3 could be a useful potential therapeutic agent for AD but it still presents potential pharmacological liabilities for drug use. While introducing unnatural ß-Alanine residues did reduce its degradation in the plasma, its intramolecular disulfide bond is still susceptible to reduction *in vivo*. Reducing the disulfide bond (breaking the bond) destabilizes the peptide's ß-hairpin conformation, thus reducing its potency. Hence, design and

2

Commented [JP1]: Include a transition here to signal to the reader that you are explaining why agonists are maybe more promising

Commented [JP2]: Include a transition her to signal to the reader that you are explaining why agonists are maybe more promising

Commented [JP3R2]:

Commented [JP4]: Include a transition here to signal to the reader that you are explaining why agonists are maybe more promising

synthesis of novel APY-d3 derivatives that are stabilized by intramolecular non-covalent interactions rather than disulfide bonds may yield an antagonistic agent with equal or greater potency than APY-d3 without redox susceptibility.

Methods

General Chemistry and Synthesis/Purification of Agents

      Fmoc-protected amino acids are necessary to guide the correct direction of coupling reactions in solid phase peptide synthesis. The majority of Fmoc-amino acids were purchased commercially, but some were synthesized within the Pellecchia Lab. Each Fmoc-protection reaction proceeded in 50 mL THF/water (1:1) with 1.1 equivalence of Fmoc-chloride in 10 mL tetrahydrofuran (THF), 1 equivalence of amino acid and 3.75 equivalence of Na_2CO_3. Fmoc-protected amino acids were purified to at least 95% purity on a silica 24g RediSep Column with a cyclohexane/ethyl acetate gradient (10% to 100%) and dried under high vacuum. All but one agent were synthesized in-house. Peptide synthesis was achieved with a Liberty Blue Peptide Synthesizer and CEM microwave reactor following standard microwave-assisted Fmoc peptide synthesis protocols on Rink amide resin. Each coupling reaction in the Liberty Blue Peptide Synthesizer used 6 equivalence of Fmoc-protected amino acid, 3 equivalence of N,N'-diisopropylcarbodiimide (DIC) and 1 equivalence of OximaPure in 3.5 mL dimethylformamide (DMF). After allowing the coupling reaction to progress for 5 minutes at 90 °C under microwave, Fmoc-protected amino acids were deprotected with a 20% piperidine in DMF (2 x 3 mL) for three minutes at 90 °C. After the final coupling reaction and washing steps, the peptides were cleaved from the Rink amide resin with a cleavage cocktail composed of trifluoroacetic acid (TFA)/triisopropylsilane (TIS)/water/phenol (94:2:2:2) for three hours. This cleavage

cocktail was filtered from the resin into diethyl ether (Et$_2$O) to precipitate the peptide, centrifuged, washed with Et$_2$O, centrifuged again and dried under high vacuum. The crude peptides were dissolved in DMSO and purified to at least 95% purity by reverse-phase high performance liquid chromatography (RP-HPLC) using an Xterra column (Waters) on a JASCO preparative HPLC system with a water/acetonitrile gradient (5% to 100%) containing 0.1% TFA. Once purified, agents were finally characterized by high resolution mass spectrometry (HRMS).

Expression and Purification of EphA4

In-house expression of EphA4 was necessary to test thermodynamics of binding to antagonistic test agents via isothermal titration calorimetry (ITC). To begin the pre-culture, 50 µL 1000x AMP was added to 50 mL sterile LB broth (sterilized by autoclave), the broth was inoculated with *E. coli* transformed with a HisEphA4-LBD encoding plasmid and then placed on a shaker at 37 °C for 16-18 hours. After shaking overnight, 1 mL 1000x AMP was added to 1000 mL of sterile LB broth along with 1 mL of the pre-culture. The culture was incubated on a shaker at 37 °C until an OD of 0.6-0.7 was achieved. At this point, 400 µL IPTG was added to induce expression of the EphA4-LBD. Induction proceeded at 20 °C for 16 hours. The induced culture was centrifuged at 5000 RPM for 20 minutes to condense cells into a pellet before the pellet was resuspended in approximately 45 mL lysis buffer (25 mM Tris pH = 8.0, 500 mM NaCl). 45 µL dithiothreitol (DTT) was added to the resuspended cell solution along with 1 tab of ETDA dissolved in 1 mL miliQ H$_2$O. This solution was sonicated for 2 iterations of 12 cycles for 6 minutes at 35% amplitude. After lysis, the solution was centrifuged at 12000 RPM for 20 minutes, the supernatant was filtered through a 0.45 µm filter and DTT was added a second time to a final concentration of 1 mM. Filtered lysate was purified on an FPLC system with a Binding

Buffer (25 mM Tris pH = 7.5, 500 mM NaCl) / Elution Buffer (25 mM Tris pH= 7.5, 500 mM NaCl, 500 mM imidazole) gradient (4% to 100%) over 60 minutes. After elution, a size-exclusion desalting column was used to isolate pure EphA4-LBD.

Biophysical Characterization of Agents

1D ^{1}H NMR experiments on APY-d3, 146H6 and 146I4 were performed by Dr. Carlo Baggio using a 700 MHz Bruker instrument equipped with a TCI cryo-probe.

Isothermal titration calorimetry (ITC) measurements were performed under very close guidance of Dr. Luca Gambini and Dr. Carlo Baggio. ITC measurements were acquired with a TA Instruments microcalorimeter to obtain the agents' thermodynamics of binding with EphA4-LBD. EphA4-LBD was dissolved in a 25 mM Tris pH = 7.5, 150 mM NaCl buffer and loaded into the syringe while the target agent, dissolved in the same buffer + 1% DMSO, was loaded into the cell. 20x2.5 µL titrations (every 200 seconds) with stirring were performed at 25 °C. Optimized binding curves for the majority of tested agents were achieved with [EphA4-LBD] = 200 µM (in the syringe) and [Test Agent] = 40 µM (in the cell). For some agents, the concentration of stock solutions used to make dilutions for ITC samples was verified using 1D ^{1}H NMR in which signal intensity was compared to spectra for solutions with known concentrations. ITC measurements of 146I4 were conducted by Dr. Luca Gambini and measurements of APY-d3 were conducted by both Dr. Luca Gambini and Dr. Carlo Baggio.

Results and Discussion

Elimination of the Disulfide Bond in APY-d3 and Optimization of Linear Peptides

Thermodynamics of binding are governed by the Gibbs free energy equation: $\Delta G = \Delta H - T\Delta S$. Isothermal titration calorimetry directly measures the power (μcal/s) required to minimize the temperature difference between the agent-containing sample cell (into which the target protein is titrated) and a reference cell maintained at constant temperature. This provides direct measurement of the enthalpy of binding (ΔH). The Gibbs free energy (ΔG) is related to the dissociation constant (K_d) of the protein-ligand binding equilibrium. This relationship is expressed as follows: $-RT\ln(1/K_d) = \Delta G$. Since isothermal titration calorimetry also provides a measurement of K_d, a value for ΔG is obtained as well. With measured ΔH and ΔG values, a value for the loss of entropy upon binding (ΔS) can be indirectly extrapolated. Molecules that present a stable pre-arranged binding conformation in solution would experience smaller losses on entropy upon binding, resulting in a higher potency.

Based on structure-based design strategies, the most promising route of stabilizing the APY-d3 derivative's ß-hairpin conformation without a disulfide bond was to replace residues Cysteine-4 and Cysteine-12 with an intramolecular hydrophobic interaction between hydrophobic residues at those positions. One SAR began by substituting alanine residues in place of the cysteine residues, yielding the linear, unconstrained peptide 146F4 (**Table 1**). ITC measurements of APY-d3 and 146F4 demonstrate that destabilization of APY-d3's ß-hairpin conformation significantly reduced the binding affinity of the resulting agent (**Figure 1 A-B**). Thermodynamics of binding for all further peptides were measured side by side with 146F4 as a control. Due to the linear, unconstrained nature of 146F4, any additional stabilization of the ß-hairpin conformation would be reflected by differing changes in entropy (ΔS) upon binding to EphA4. To optimize the intramolecular hydrophobic interaction, α-aminobutyric acid, valine, isoleucine and leucine residues were systematically introduced at positions 4 and 12 (**Table 1,**

6

146G2-146G9). While larger hydrophobic residue substitutions at position 4 appeared to reduce binding affinity for EphA4, leucine and isoleucine substitutions at position 12 yielded peptides 146G5 and 146G6 respectively, each with slightly improved binding affinity compared to 146F4 (**Table 1**).

Further structure-based design analysis of APY in the EphA4 ligand binding domain (EphA4-LBD) revealed an arginine residue adjacent to positions 12 and 11. A progression was pursued in which position 12 was substituted with negatively charged residues glutamate and aspartate, as well as other residues known to associate favorably with arginine such as tryptophan and threonine (**Table 1, 146G11-146H2**). Additionally, serine-11 was substituted with D-amino acids in an attempt to rotate the side chain of residue-11 toward the arginine, but this progression yielded agents less effective than 146F4 (**Table 1, 146H3-146H5**). 3D modeling revealed a second arginine residue in the EphA4-LBD adjacent to position 9. Substituting serine-9 with a negatively charged glutamate while leaving a hydrophobic leucine or isoleucine residue at position 12 appeared to optimize this arginine-sidechain interaction while retaining the ß-hairpin stabilization gained from the intramolecular hydrophobic interaction between residues 4 and 12 (**Table 1, 146H10 & 146H6**). This yielded peptide 146H6, which was built off of in additional SAR studies.

EphA4 contains a hydrophobic bed in its LBD, which may in part explain the increased binding affinity of peptides whose ß-hairpins are stabilized by intramolecular hydrophobic interactions. Thus, another SAR was pursued in which arginine-7 was substituted with progressively more hydrophobic residues. Alanine, valine, leucine and phenylalanine at position 7 all appeared to reduce binding affinity, however inserting a leucine reduced binding affinity the

least (**Table 1, 146H12-146I3**). 146I2 may be a possible alternative antagonistic agent to optimize in the future.

ID	Sequence	Kd (nM)
APY-d3	H$_2$N-(ßA)PY**C**VYR(ßA)SWS**C**-CONH$_2$	42.2
146F4	H$_2$N-(ßA)PY**A**VYR(ßA)SWS**A**-CONH$_2$	673 ± 35.6, n = 16
146G2	H$_2$N-(ßA)PY**V**VYR(ßA)SWSA-CONH$_2$	1930 ± 710, n = 2
146G3	H$_2$N-(ßA)PYAVYR(ßA)SWS**V**-CONH$_2$	362 ± 74.1, n =3
146G4	H$_2$N-(ßA)PY**V**VYR(ßA)SWS**V**-CONH$_2$	2980 ± 150, n = 2
146G5	H$_2$N-(ßA)PYAVYR(ßA)SWS**I**-CONH$_2$	510 ± 51, n = 2
146G6	H$_2$N-(ßA)PYAVYR(ßA)SWS**L**-CONH$_2$	424 ± 152, n =3
146G9	H$_2$N-(ßA)PY(**α-Abu**)VYR(ßA)SWS**L**-CONH$_2$	1300
146G11	H$_2$N-(ßA)PYAVYR(ßA)SWS**E**-CONH$_2$	534
146G12	H$_2$N-(ßA)PYAVYR(ßA)SWS**D**-CONH$_2$	493
146H1	H$_2$N-(ßA)PYAVYR(ßA)SWS**W**-CONH$_2$	768
146H2	H$_2$N-(ßA)PYAVYR(ßA)SWS**T**-CONH$_2$	554
146H3	H$_2$N-(ßA)PYAVYR(ßA)SW(**D-Ser**)**L**-CONH$_2$	1980
146H4	H$_2$N-(ßA)PYAVYR(ßA)SW(**D-Glu**)**L**-CONH$_2$	2530
146H5	H$_2$N-(ßA)PYAVYR(ßA)SW(**D-Asp**)**L**-CONH$_2$	1060
146H7	H$_2$N-(ßA)PYAVYR(ßA)**D**WS**L**-CONH$_2$	428
146H8	H$_2$N-(ßA)PYAVY**K**(ßA)**E**WS**L**-CONH$_2$	877
146H12	H$_2$N-(ßA)PYAVY**A**(ßA)**E**WS**L**-CONH$_2$	2170
146I1	H$_2$N-(ßA)PYAVY**V**(ßA)**E**WS**L**-CONH$_2$	2150
146I3	H$_2$N-(ßA)PYAVY**F**(ßA)**E**WS**L**-CONH$_2$	772
146I2	H$_2$N-(ßA)PYAVY**L**(ßA)**E**WS**L**-CONH$_2$	486
146H10	H$_2$N-(ßA)PYAVYR(ßA)**E**WS**I**-CONH$_2$	355
146H6	H$_2$N-(ßA)PYAVYR(ßA)**E**WS**L**-CONH$_2$	364 ± 49, n = 3

Table 1. Tested Agents and K$_d$ Values (nM) from ITC. Standard errors represent the variations between the indicated multiple (n) measurements. α-Abu, α-aminobutyric acid.
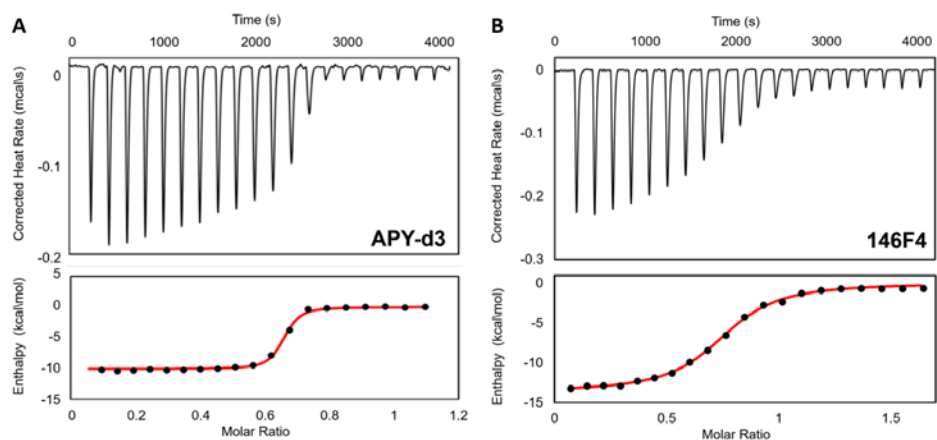
Figure 1. ITC Curves for Binding Between EphA4-LBD and (A) APY-d3 (ΔH = -10.05

kcal/mol, -TΔS = -0.011 kcal/mol), **(B)** 146F4 (ΔH = -12.70 ± 0.20 kcal/mol, -TΔS = 4.31 ± 0.22

kcal/mol).

Replacement of ß-Alanine in Position 8 with Constrained Amino Acids

The flexible ß-alanine residue at position 8 in APY-d3 grants the peptide the rotational degrees of freedom necessary for the peptide to fold into its ß-hairpin conformation. The linear, non-constrained APY-d3 derivative 146F4 retains this ß-alanine residue, but without the disulfide bridge stabilizing the ß-hairpin into the correct conformation, the peptide must undergo significant organization upon binding to EphA4-LBD. This transition to an organized state, i.e. a negative change in entropy, is unfavorable, thereby decreasing binding affinity. Through structure-based design strategies, it was hypothesized that substituting this flexible ß-alanine at position 8 with a more constrained amino acid would force the agent into a ß-hairpin conformation without introducing additional rotational degrees of freedom. All but one of these substitutions demonstrated close to or greater than 10^4 nM binding affinity or were completely inactive with EphA4 (**Table 2, 146F7-146F12**). However, the constrained amino acid introduced to position 8 in the peptide 146I4 resulted in the highest affinity antagonistic agent produced in this study so far (**Table 2, 146I4**). 146I4 combines the constrained amino acid substitution with optimizations achieved from previous SARs, interacting favorably with an adjacent arginine residue and is further stabilized in its ß-hairpin conformation via an intramolecular hydrophobic interaction. While the majority of 146I4's sequence is presented in Table 2, the identity of the constrained amino acid in position 8 is preferred to not be publicly disclosed until further studies are performed that could result in a patent application by UCR.

146I4's more structured nature in solution before binding was affirmed through a 1D ^{1}H NMR experiment, comparing the proton chemical shifts between APY-d3, 146H6 and 146I4 (**Figure 2**). It was observed that for 146H6, proton chemical shifts are grouped together with little dispersion between peaks. This is because 146H6 is relatively unstructured in solution; the

majority of protons are exposed to solvent and thus all share a similar chemical environment. With variation in electron shielding arising only from differences in residue sidechains, there is little variation in the chemical shifts observed. On the other hand, the ^{1}H NMR spectra for both APY-d3 and 146I4 show a more spread-out, diverse range of chemical shifts. APY-d3 is known to be structured in solution due to the covalent disulfide bond that stabilizes the agent into a ß-hairpin conformation. Some protons are internalized into the ß-hairpin 3D structure while others are exposed to solvent, so protons are exposed to a more diverse set of chemical environments, resulting in a wider range of chemical shifts. The ^{1}H NMR spectrum of 146I4 more closely matches that of APY-d3 than 146H6, suggesting that 146I4 is stabilized in a structured ß-hairpin conformation before binding to EphA4-LBD. 146I4's ß-hairpin stabilization is further confirmed through ITC measurements between EphA4-LBD and 146H6 versus EphA4-LBD and 146I4 (**Figure 3 A-B**). The negative ΔS observed upon binding of 146H6 reflects that the agent must organize itself to fit into the EphA4 binding pocket (**Figure 3 A**). In contrast, 146I4 actually exhibits a positive ΔS on binding (**Figure 3 B**). This provides insight into 146I4's entropically-driven binding to EphA4-LBD.
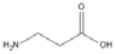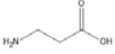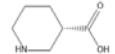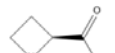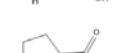
ID	Residue 8 Structure	Sequence	Kd (nM)
APY-d3		H$_2$N-(ßA)PY**C**VYR(ßA)SWS**C**-CONH$_2$	42.2
146F4		H$_2$N-(ßA)PY**A**VYR(ßA)SWS**A**-CONH$_2$	673 ± 35.6, n = 16
146F7		H$_2$N-(ßA)PYAVYR(**3-Az**)SWSA-CONH$_2$	Inactive
146F8		H$_2$N-(ßA)PYAVYR(**L-ß-Pro**)SWSA-CONH$_2$	> 10^4, n = 2
146F9		H$_2$N-(ßA)PYAVYR(**L-Nip**)SWSA-CONH$_2$	8100
146F10		H$_2$N-(ßA)PYAVYR(**L-2-Az**)SWSA-CONH$_2$	Inactive
146F11		H$_2$N-(ßA)PYAVYR(**D-2-Az**)SWSA-CONH$_2$	> 10^4, n = 2
146F12		H$_2$N-(ßA)PYAVYR(**D-β-Pro**)SWSA-CONH$_2$	> 10^4
146I4	**?**	H$_2$N-(ßA)PYAVYR(**?**)**E**WS**L**-CONH$_2$	304

Table 2. Tested Agents with Residue 8 Substitutions and K$_d$ Values (nM) from ITC.
Standard errors represent the variations between the indicated multiple (n) measurements.
"Inactive" indicates failure to produce a binding curve when measured by ITC. 3-Az, 3-azetidinecarboxylic acid; L-Nip, L-nipecotic acid; L-2-Az, L-azetidine-2-carboxylic acid; D-2-Az, D-azetidine-2-carboxylic acid; The amino acid indicated with a question mark cannot be disclosed at this point to not preclude the possibility of filing a patent application by UCR.
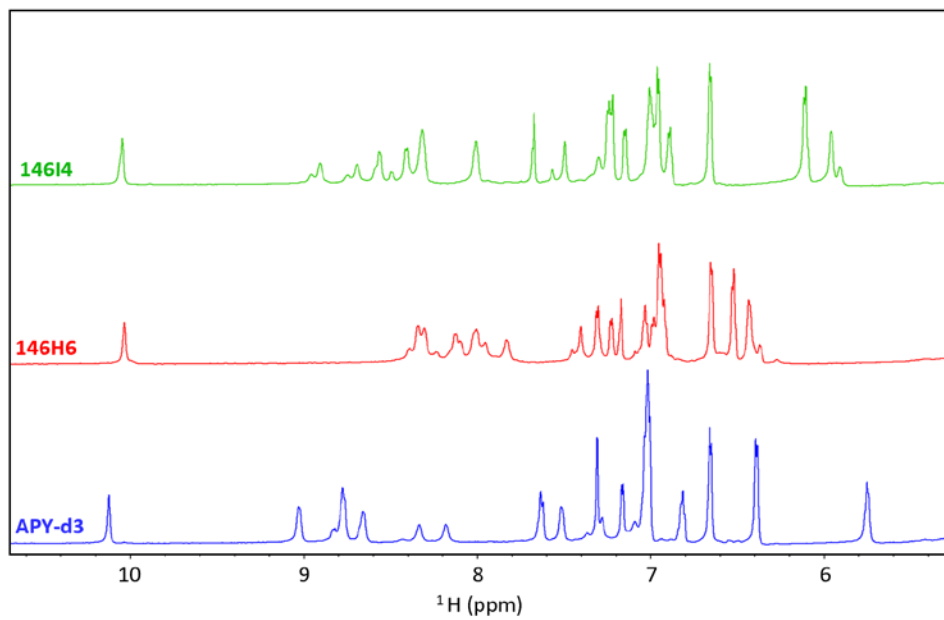
12

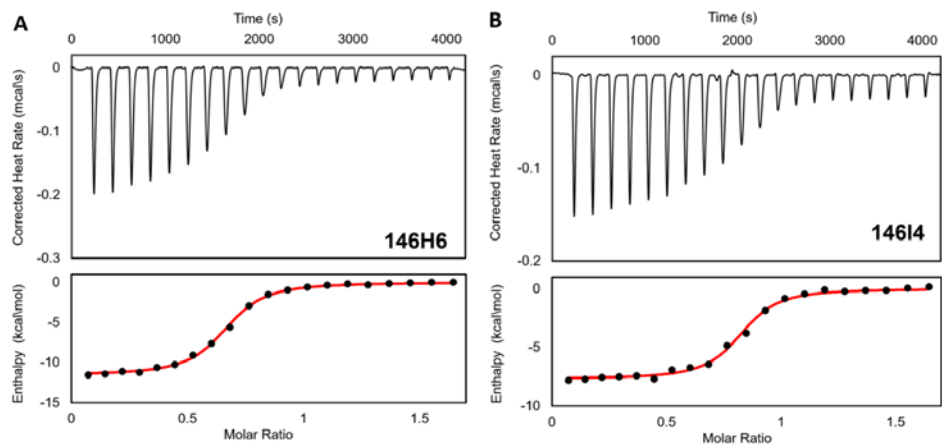**Figure 2. 1D ^{1}H NMR Spectra (amide and aromatic regions) for APY-d3, 146H6 and 146I4**.

Figure 3. ITC Curves for Binding Between EphA4-LBD and (A) 146H6 (ΔH = -11.32 ± 0.34

kcal/mol, -TΔS = 2.52 ± 0.41 kcal/mol), **(B)** 146I4 (ΔH = -7.70 kcal/mol, -TΔS = -1.19

kcal/mol).

Conclusions

Although 146I4 does not demonstrate a binding affinity on the same order of magnitude as APY-d3, an antagonistic agent for EphA4 with a ß-hairpin conformation stabilized through means other than an intramolecular disulfide bond was successfully produced. 146I4 successfully combines the stabilizing effects of intramolecular hydrophobic interactions and a constrained amino acid to force the agent into a ß-hairpin conformation. Additionally, binding affinity of this constrained agent was improved via manipulating sidechain interactions with charged amino acids and a hydrophobic bed in the EphA4-LBD. Analysis of PDB protein-protein complexes has shown that ß-hairpins are essential conformations to thousands of protein-protein interactions (Watkins and Arora, 2014). Thus, producing stable ß-hairpins is highly sought-after in the discovery of pharmaceuticals. We hope that the design of 146I4, particularly the constrained amino acid inserted at position 8, may serve as a novel technique of satisfying this demand for ß-hairpin stabilization in more widespread drug discovery across the industry.

15

References

Fu, A. K., Hung, K., Huang, H., Gu, S., Shen, Y., Cheng, E. Y., . . . Ip, N. Y. (2014). Blockade
   of EphA4 signaling ameliorates hippocampal synaptic dysfunctions in mouse models of
   Alzheimer's disease. *Proc. of the Nat. Acad. of Sci., 111*(27), 9959-9964.
   doi:10.1073/pnas.1405803111

Murai, K. K., Nguyen, L. N., Koolpe, M., Mclennan, R., Krull, C. E., & Pasquale, E. B. (2003).
   Targeting the epha4 receptor in the nervous system with biologically active peptides. *Mol.
   and Cell Neurosci., 24*(4), 1000-1011. doi:10.1016/j.mcn.2003.08.006

Olson, E. J., Lechtenberg, B. C., Zhao, C., Torre, E. R., Lamberto, I., Riedl, S. J., . . . Pasquale,
   E. B. (2016). Modifications of a Nanomolar Cyclic Peptide Antagonist for the EphA4
   Receptor To Achieve High Plasma Stability. *ACS Med. Chem. Lett., 7*(9), 841-846.
   doi:10.1021/acsmedchemlett.6b00132

Pasquale, E. B. (2008). Eph-ephrin bidirectional signaling in physiology and disease. *Cell 133*,
   38-52

Poppe, Lindsay, et al. "EphA4 Loss Improves Social Memory Performance and Alters Dendritic
   Spine Morphology without Changes in Amyloid Pathology in a Mouse Model of
   Alzheimer's Disease." *Alzheimer's Research & Therapy*, vol. 11, no. 1, 2019,
   doi:10.1186/s13195-019-0554-4.

Sawyer, N., & Arora, P. S. (2018). Hydrogen Bond surrogate stabilization Of β-hairpins. *ACS
   Chem. Bio., 13*(8), 2027-2032. doi:10.1021/acschembio.8b00641

Van Hoecke A, Schoonaert L, Lemmens R, et al. EPHA4 is a disease modifier of amyotrophic
   lateral sclerosis in animal models and in humans. *Nat Med.* 2012;18(9):1418-1422.
   doi:10.1038/nm.2901

16

Vargas, Cerpa, W., Muñoz, F., Zanlungo, S., & Alvarez, A. (2018). Amyloid-β oligomers

    Synaptotoxicity: The emerging role OF EphA4/c-Abl signaling in Alzheimer's disease.

    Biochimica Et Biophysica Acta (BBA) – Mol. Bas. of Disease, 1864(4), 1148-1159.

    doi:10.1016/j.bbadis.2018.01.023

Wu, B., De, S. K., Kulinich, A., Salem, A. F., Koeppen, J., Wang, R., . . . Pellecchia, M. (2017).

    Potent and Selective EphA4 Agonists for the Treatment of ALS. *Cell Chem. Bio., 24*(3),

    293-305. doi:10.1016/j.chembiol.2017.01.006